Science of the Total Environment 407 (2009) 5319–5327

Contents lists available at ScienceDirect

Science of the Total Environment

journal homepage: www.elsevier.com/locate/scitotenv

Characterization of winter airborne particles at Emperor Qin's Terra-cotta Museum, China

Tafeng Hu [a,b,c,*], Shuncheng Lee [c], Junji Cao [a,b], Judith C. Chow [b,d], John G. Watson [b,d], Kinfai Ho [c], Wingkei Ho [c], Bo Rong [e], Zhisheng An [b]

[a] Department of Environmental Science and Engineering, Xi'an Jiaotong University, Xi'an, 710049, China
[b] SKLLQG, Institute of Earth Environment, Chinese Academy of Sciences, Xi'an, 710075, China
[c] Department of Civil and Structural Engineering, The Hong Kong Polytechnic University, Hong Kong, China
[d] Division of Atmospheric Sciences, Desert of Research Institute, Reno, USA
[e] Emperor Qin's Terra-cotta Warriors and Horses Museum, Xi'an, China

ARTICLE INFO

Article history:
Received 12 December 2008
Received in revised form 15 June 2009
Accepted 25 June 2009
Available online 28 July 2009

Keywords:
Total suspended particles
Indoor air
Visitor number
SEM-EDX
Museum

ABSTRACT

Daytime and nighttime total suspended particulate matters (TSP) were collected inside and outside Emperor Qin's Terra-cotta Museum, the most popular on-site museum in China, in winter 2008. The purpose of this study was to investigate the contribution of visitors to indoor airborne particles in two display halls with different architectural and ventilating conditions, including Exhibition Hall and Pit No.1. Morphological and elemental analyses of 7-day individual particle samples were performed with scanning electron microscopy and energy dispersive X-ray spectrometer (SEM-EDX). Particle mass concentrations in Exhibition Hall and Pit No.1 were in a range of 54.7–291.7 $\mu g\,m^{-3}$ and 95.3–285.4 $\mu g\,m^{-3}$ with maximum diameters of 17.5 μm and 26.0 μm, respectively. In most sampling days, daytime/nighttime particle mass ratios in Exhibition Hall (1.30–3.12) were higher than those in Pit No.1 (0.96–2.59), indicating more contribution of the tourist flow in Exhibition Hall than in Pit No. 1. The maximum of particle size distributions were in a range of 0.5–1.0 μm, with the highest abundance (43.4%) occurred in Exhibition Hall at night. The majority of airborne particles at the Museum was composed of soil dust, S-containing particles, and low-Z particles like soot aggregate and biogenic particles. Both size distributions and particle types were found to be associated with visitor numbers in Exhibition Hall and with natural ventilation in Pit No.1. No significant influence of visitors on indoor temperature and relative humidity (RH) was found in either display halls. Those baseline data on the nature of the airborne particles inside the Museum can be incorporated into the maintenance criteria, display management, and ventilation strategy by conservators of the museum.

1. Introduction

The discovery of Emperor Qin's terra-cotta warriors and horses, Xi'an, China, in 1974 was one of the most important archeological finding of the 20th century. Today, terra-cotta warriors and horses inside the largest on-site museum in China are recognized as "The Eighth Wonder of the World" (http://www.bmy.com.cn). More than 2 million tourists visit the museum each year for the fabulous terra-cotta army in full battle array in one of the on-site exposed pits, Pit No. 1 (Pit 1), and the bronze chariots and horses in *E*xhibition *H*all (EH). Since excavation, these priceless and irreplaceable statues have undergone changes in their appearance after more than 30-years of exposure in the display halls (Zhang, 1998; Cao et al., 2005). The Emperor Qin's Terra-cotta Warriors and Horses Museum (referred as Museum) founded in 1979 is located in a suburb environment, 30 km to the east of Xi'an, a city of eight million population with increasing traffic, high coal consumption, and intensive construction. A power plant is located 17 km west of the Museum and a highway is located 5 km north of the Museum. The Museum is also surrounded by agricultural fields in which biomass are periodically burned in summer and autumn.

The conservation of cultural heritage and its protection against possible damage from air pollution is of increasing scientific concern (Brimblecombe, 1990, 2003). Air pollution can cause chemical damage or soiling of surfaces due to particle deposition or absorption of gases (De Bock et al., 1995; Van Grieken et al., 1998; Godoi et al., 2006). Once particles deposit on work of art, their appearances and chemical interactions with the surface depend on their chemical composition and morphology (Nazaroff et al., 1993; Potgieter-Vermaak et al., 2005). Investigations on calcareous stone weathering show that physical stress from soluble salt crystallization in pores caused stone breakage (Cardell et al., 2003). It is suggested that visitors entering the buildings are responsible for transferring particulate materials inside or re-

* Correspondence author. Department of Environmental Science and Engineering, Xi'an Jiaotong University, Xi'an, Shaanxi, China. Tel.: +86 29 8266 8385; fax: +86 29 8266 8789.
E-mail addresses: hutafeng@hotmail.com, cao@loess.llqg.ac.cn (T. Hu).

0048-9697/$ – see front matter © 2009 Elsevier B.V. All rights reserved.
doi:10.1016/j.scitotenv.2009.06.044

suspending the deposited dust from the floor and pavement. Thatcher and Layton (1995) found that people walking in a room could double the atmospheric particle concentration. Yoon and Brimblecombe (2000) noted that shoes and clothing were a major source of indoor dusts. Previous studies also showed that visitor flow was a major contributor to soiling (Yoon and Brimblecombe, 2001; Godoi et al., 2008) and changes of microclimate (Camuffo et al., 2001; Sanchez-Morala et al., 2005).

The aim of this study was to investigate the contribution of tourist flow on the transport and deposition of indoor airborne particles in two display halls with different tightness of structure, as well as their aerosol chemical compositions. Size distribution, morphology, and elemental composition of approximately 8000 individual particles were analyzed using SEM-EDX to examine their possible sources, potential soiling and weathering hazards to the artifacts. Guidelines and recommendations for the improvement of indoor environment in this on-site museum can be established on the base of the present results.

2. Sampling

2.1. Sample collection

Airborne TSP samples were collected during Chinese Lunar Spring Festivals from 15 to 22 February 2008. The sampling campaign was organized at three separate sampling sites marked with red stars in Fig. 1. One sampling site is at the western part of Pit 1, the largest display hall of the Museum opened to public since 1979. One sampling site is positioned in EH, opened to public since 1999. The differences of the two sampling sites are the building structure and ventilation. Pit No.1 is covered with a hangar-like steel-frame vault to shield the statues from direct solar illumination and precipitation. All the wide windows in Pit 1 remain open all year long. There is no window in the Exhibition Hall. This display hall is equipped with mechanical ventilation and air-conditioning system, but the system only operate in about 30 hot days in summer due to economic and maintenance reasons. The air mass exchanges in EH were only through the entrance of the hall and narrow cracks in the building shell. The outdoor sampling site is located on the roof of the Museum's office building, about 10 m above the ground.

Sampling at above three sites was carried out simultaneously in order to obtain a comparative result of the measurement. In winter, the Museum is opened to the public from 8:30 a.m. to 5:00 p.m. The daytime samples in this study were collected from 10:00 a.m. to 3:00 p.m., representative of indoor airborne particles with the influence of visitor activities. The nighttime samples were collected from 11:00 p.m. to 4:00 a.m. in the next morning, representative of indoor airborne particles without influence of visitors. Since considerable coarse particles larger than 10 μm had been detected in indoor aerosols (Cao et al., 2005), in this study TSP samples were collected onto 47 mm polycarbonate Nuclepore filters (0.4 μm in porosity; Whatman International Ltd., Maidstone, UK) using mini-vol air samplers (Airmetrics Corp., Springfield, OR, USA) with an operating flow rate of 5 $L\,min^{-1}$. Under pre-optimized 5-hour sampling duration, particles were collected in a single layer onto the filters with minimal particle-to-particle contact. After sampling, filters were placed in plastic cassettes and stored in a refrigerator at 4 °C until analyzed.

2.2. Sample measurement

Small rectangular sections (approximately 10 × 10 mm) were cut from the TSP Nuclepore filters and mounted on the holder with conductive adhesive carbon tape. Samples were coated under vacuum with gold and analyzed using a computer-controlled JEOL JSM-6460 LV SEM (Japan Electron Optics Laboratory Co. Ltd., JP) under 20–25 kV accelerating voltage at a work distance of 10 mm. For each sample, ten secondary electron images (SEI) were acquired with magnifications from 1000× to 5000×, depending on the particle size in respective image views. The diameter of each individual particle was measured from SEI images by commercial IMAGE PRO PLUS 5.0 (Media Cybernetics, Inc., Silver Spring, MD, USA) processing and analysis software (Ingham et al., 2000; Germain et al., 2003; Sheu et al., 2005; Tian et al., 2006; Yue et al., 2006). The image software is capable of automatically identifying each object against the background and providing measurements of such geometric properties as the projected area, perimeter, and the maximum and minimum caliper lengths. The

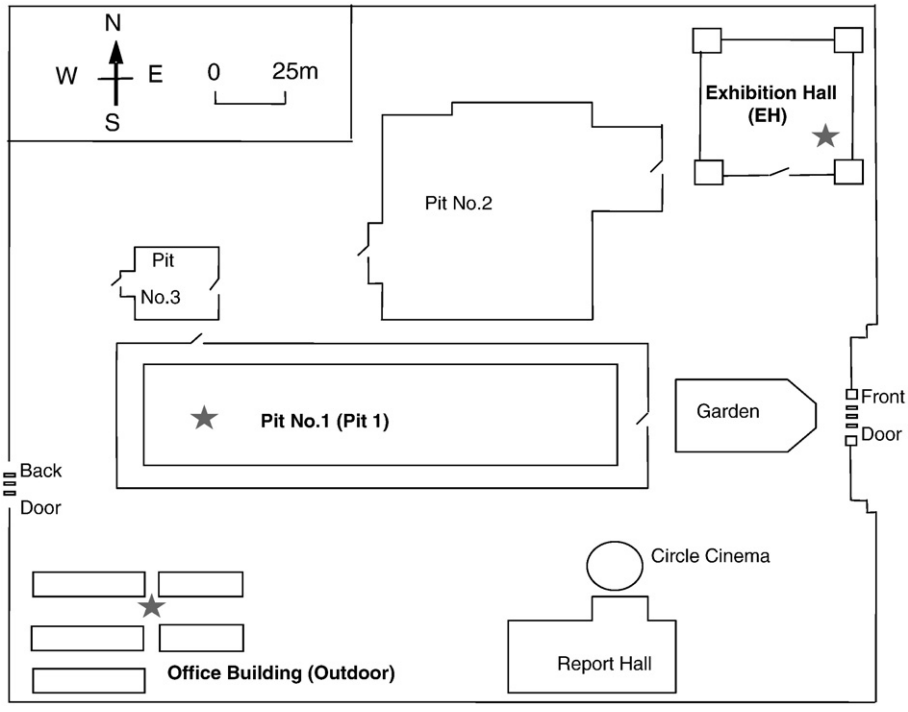

Fig. 1. The three sampling locations in EH, in Pit 1, and on the roof of office building (outdoor) are marked with red stars.

images were processed with median filtering to remove impulse noise (Tansel and Nagarajan, 2004). The diameter of a particle was estimated as the average of the longest dimension and its orthogonal width (Zhang et al., 2003; Okada and Kai, 2004). All particles with a diameter larger than 0.2 μm in each image were measured to obtain general size distributions. Individual particles larger than 0.5 μm in each sample were selected for elemental analyses manually using NORAN SYSTEM SIX Si–Li EDX detector with an ultra thin window (Thermo Electron Corporation, Waltham, MA, USA). In previous studies, EDX acquisition time differed significantly, ranging from 5 s to 120 s (Betzer et al., 1988; Ghermandi et al., 1999; Trochkine et al., 2003; Dalia Pereira et al., 2004; Okada and Kai, 2004). During our optimization experiments under different acquisition time at magnifications from 1000× to 20,000×, more elements were detected under longer acquisition time, with the relative contents of those additional elements no more than 5%, ranging from 0.01% to 4.98%. Since the particle classification in this study was based on the content of the most abundant elements, the EDX acquisition time was 30 s live-time for each particle at magnifications of 1000×, 3000× and 5000×, according to particle size in respective images. Nearly 200 particles in each sample were measured. X-ray peak intensities for each element were converted into atomic and weight fractions using the EDX software without ZAF correction.

Nuclepore polycarbonate filters were analyzed gravimetrically for mass concentrations by means of a Sartorius MC5 electronic microbalance with a ±1 μg sensitivity (Sartorius, Göttingen, Germany). Meteorological conditions were recorded using a Davis Vantage Pro2 weather station (Davis Ins., Hayward, CA, USA) positioned at the outdoor site. Indoor temperature and relative humidity records were provided by two Testo infrared sensors (175H2 and 177H1, Testo Inc., Germany). Visitor numbers were obtained from the records held by the managers of the Museum.

3. Results and discussion

3.1. Microclimate

The site of the museum belongs to semi-arid and semi-humid continental climate with the lowest temperature and rare precipitation in winter. The meteorological conditions in the 7-day sampling campaign are similar and representative of the winter in North China, with the speeds of prevailing west-southwesterly wind ranging from 0.2 to 1.3 $m\,s^{-1}$. The variation of temperature and RH at the three sampling sites is shown in Fig. 2. The outdoor temperature was between −1.1 °C and 18.4 °C in the sampling days, and the RH ranged from 19% to 78%. Indoor temperature in Pit 1 was between −1.2 °C and 13 °C, a little lower than those outdoors; however, the indoor RH was between 34% and 99%, much higher than the concurrent outdoor RH. Although the heating system in EH was never operated, indoor temperature was stable in the sampling period (7.9 °C to 11.4 °C) due to the protection by thick walls, whilst the fluctuation of RH (12%–87%) followed the trend of those outdoors. In the absence of indoor heating, the temperature in Pit 1 rose steadily since 10:00 a.m. and reached the climax at about 16:00 p.m., while during the same period indoor RH descended and reached its lowest value in the afternoon. Visitors can release vapor and heat according to previous observations (Camuffo et al., 2001; Sanchez-Morala et al., 2005), but in this study no significant association between visitor flow and indoor temperature and relative humidity was found in the two display halls. As recorded in Pit 1, indoor temperature below freezing-point appeared in more than 20 days in 1989 and in 1992 (Zhang, 1998), and in 33 days in 2007. The lowest average temperature and highest relative humidity recorded in Pit 1 are supposed to be the result of better thermal conductivity performance of building materials. The temperature of steel and glass materials in Pit 1 was always lower than dew temperature at night, inducing water condensation on the surfaces. When the temperature rose the condensed water evaporated and consequently increased the indoor relative humidity. This aggressive environment in Pit 1 may promote the deterioration of terra-cotta materials through not only frequent freezing–thawing cycles in winter, but also feasible adsorption of gas pollutants on the surface of statues with high humidity. With the fluctuation of indoor RH, such physical weathering as dissolution, hydration, and crystallization of soluble salts deposited on the surface of artifacts may occur.

3.2. Mass concentrations of TSP

The daytime and nighttime samples in this study are representative collections with and without influence of visitor activities, respectively. Daytime particle mass concentrations in EH, Pit 1, and at outdoor site are in a range of 108.1–291.7 $\mu g\,m^{-3}$, 131.4–285.4 $\mu g\,m^{-3}$, 205.3–395.4 $\mu g\,m^{-3}$, whilst those nighttime mass concentrations are 54.7–173.2 $\mu g\,m^{-3}$, 95.3–260.7 $\mu g\,m^{-3}$, and 203.3–341.3 $\mu g\,m^{-3}$, respectively. Despite the great variability of measurements, the indoor values in this study are much higher than those monitored in Royal Museum of Wawel Castle in Poland, ranging from 22 to 130 $\mu g\,m^{-3}$ (Worobiec et al., 2008). Compared with that in the museum of London equipped with air-condition system (Cassar et al., 1999), the highest TSP concentration in EH is 2.5 times higher, and the highest TSP concentration in Pit 1 is a little lower than the maximum value of 303 $\mu g\,m^{-3}$ in the naturally ventilated Bethnal Green Museum located in a highly-polluted urban environment (Cassar et al., 1999). EDXRF analysis on bulk samples collected in two museums in Haque also showed higher concentrations of all elements in a museum with a structure open to the outdoor air (Kontozova-Deutsch et al., 2008). The average particle mass concentration in Pit 1 of 220.6 $\mu g\,m^{-3}$ is slightly lower than a 5-day average concentration of 360 $\mu g\,m^{-3}$, recorded in Pit 1 in January 1994 (Zhang, 1998), and a little higher than a 7-day average value of 172.4 $\mu g\,m^{-3}$, recorded in August 2004 (Cao et al., 2005).

The ratios of daytime to nighttime mass concentrations of TSP at the three sites and visitor numbers in each sampling day are illustrated in Fig. 3. Daytime/nighttime TSP ratios in EH, ranging from 1.30 to 3.12, are higher than those in Pit 1 (0.96–2.59) and outdoors (0.68–1.79) in most sampling days, indicating a larger contribution of the tourist flow on TSP concentrations in EH than in Pit 1. In EH, soil dusts were stirred up by visitors at daytime, and some coarse particles deposited at nighttime by gravitational settling onto indoor surfaces. In Pit 1 those coarse particles were still driven by airflow through the opened windows at nighttime. Compared to EH site, TSP in Pit 1 did not synchronize with the visitor fluctuation due to the influence of free air mass exchanged through wide windows.

The indoor–outdoor ratios of TSP in EH and Pit 1 indicated an obvious infiltration of outdoor particles. As shown in Table 1, only two I/O ratio values are larger than 1. Both of them were obtained at daytime, 1.22 from EH on 15 Feb and 1.05 from Pit 1 on 22 Feb, due to cleaning activities in the Museum. Although Pit 1 is a famous in-situ museum in China and terra-cotta statues are exhibited directly on the loess soil, most of the I/O ratios are smaller than 1, indicating outdoor penetration of indoor particles at both sites. The meteorological conditions were similar during the sampling days. Besides the absence of visitor activities, the large doors were closed in both EH and Pit 1 at night. This may be the reason that the I/O mass ratios at daytime are larger than those at nighttime in most sampling days. In addition, all windows in Pit 1 lead to high air exchange rates (Table 1) even when the building is closed, as well as there is no window in EH, resulting in nighttime I/O mass ratios at Pit 1 are higher than those in EH. The soiling of works of art due to deposition of airborne particles poses a hazard to museum exhibits. Over long periods of time, dark deposits build up on the surfaces of statues necessitating cleaning procedures that may be expensive and that may pose some abrasive risk to the statues. Efficient particle filtration system should consequently be employed to reduce the penetrating of outdoor particles into the buildings.

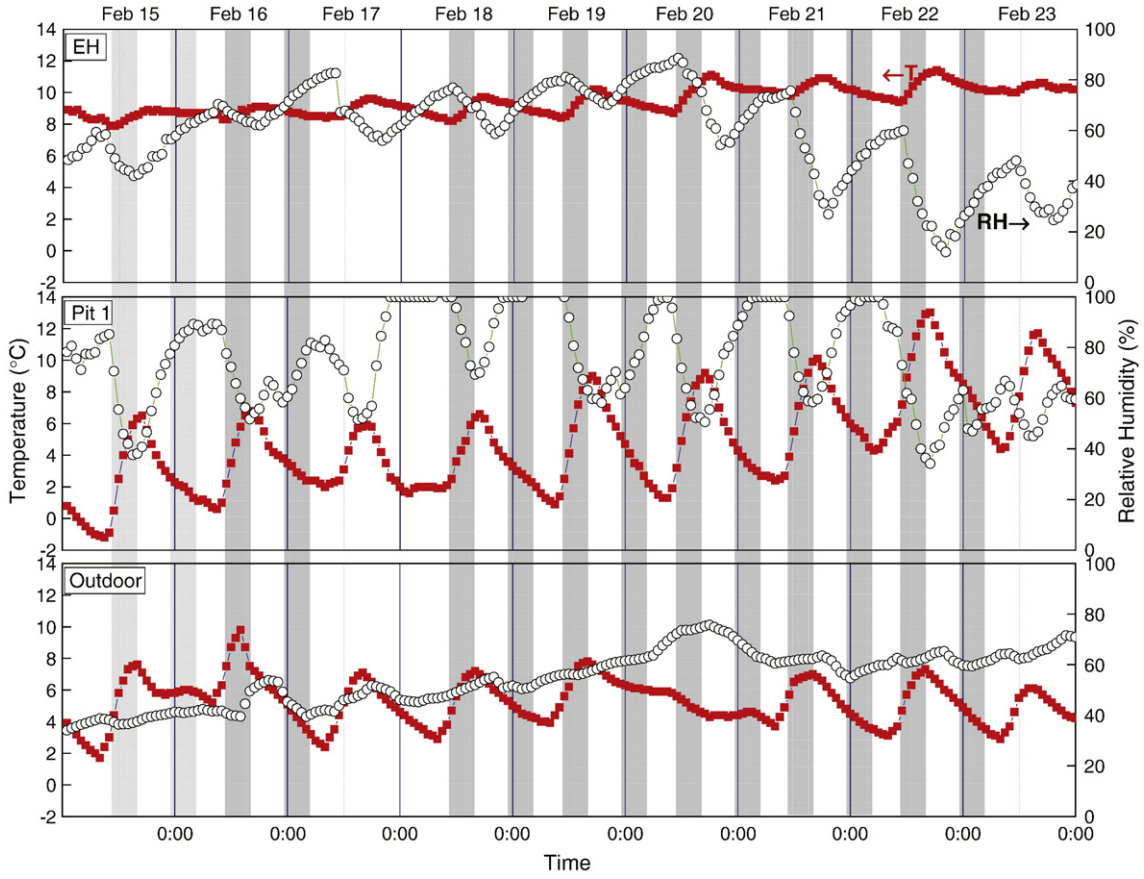

Fig. 2. From the top are temperature (red square) and relative humidity (black circle) recorded in EH, in Pit 1, and outdoors in the Museum. The grey shadows illustrate the sampling hours, including daytime sampling from 10:00 a.m. to 15:00 p.m. and nighttime sampling from 23:00 p.m. to 4:00 a.m. in the next day. (For interpretation of the references to colour in this figure legend, the reader is referred to the web version of this article.)

3.3. Particle size distribution

The number-size distribution of individual particles in the three sites measured from the SEM images is shown in Fig. 4. The maximum diameter of daytime particles collected in EH, Pit 1, and outdoors are 17.5 μm, 26.0 μm, and 26.4 μm, whilst the maximum diameter of nighttime particles are 14.3 μm, 16.2 μm, and 19.4 μm, respectively. During the seven sampling days, the wind speeds at daytime and nighttime were similar, ranging from 0.2 to 1.3 m s^{-1}. All windows were opened in Pit 1 with good air exchange rate. There is no window in EH, and air exchange in EH at night was only though the narrow crack in the building, resulting in more coarse particles suspended inside Pit 1 than inside EH all the day. Nighttime indoor particles are smaller than daytime particles in respective buildings because all doors were closed and there was no human activity at night. At all sampling sites, the measured particles are mainly 0.2–2.5 μm in size. Particles beyond this range accounted for less than 15% (shown in Fig. 4). The peaks of the size distributions at the three sites were all between 0.5 μm and 1.0 μm, among which the nighttime peak in EH and in Pit 1 had the highest (43.4%) and the second highest number percentages (41.2%), indicating more tourist disturbance on the size distribution in EH. Without visitor movement at nighttime, a few soil dusts could still be transported by the

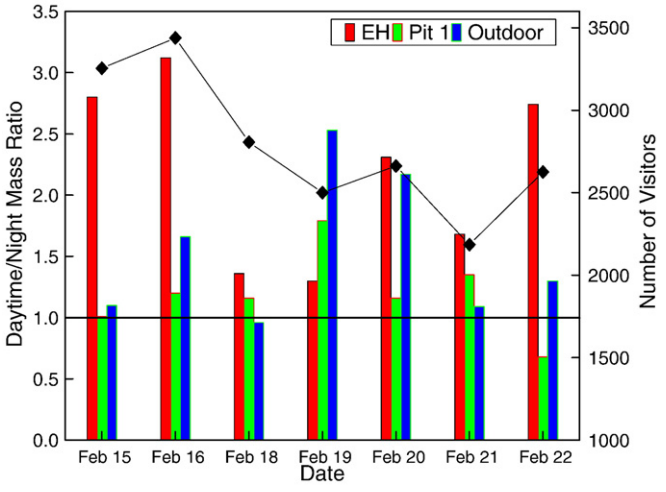

Fig. 3. The daytime/nighttime mass concentration ratios of airborne particles collected in EH, in Pit 1, and outdoors in the Museum. The black diamonds illustrate the number of visitors entered the Museum during the sampling campaign.

Table 1
Indoor/outdoor ratios of TSP in EH and Pit 1, air change rate, and the visitor numbers during the sampling days.

	Indoor/outdoor ratio of mass concentration				Visitor number
	EH, Daytime	EH, Nighttime	Pit 1, Daytime	Pit 1, Nighttime	
Feb 15	1.22	0.44	0.64	0.58	3255
Feb 16	0.74	0.28	0.81	0.58	3439
Feb 18	0.29	0.25	0.56	0.68	2806
Feb 19	0.3	0.41	0.66	0.47	2501
Feb 20	0.74	0.37	0.83	0.44	2662
Feb 21	0.44	0.35	0.72	0.89	2186
Feb 22	0.71	0.18	1.05	0.55	2626
Air change rate (h^{-1})[a]	0.40	0.12	0.65	0.24	

[a] Air change per hour was obtained from carbon dioxide tracer test for a 24-hour period.

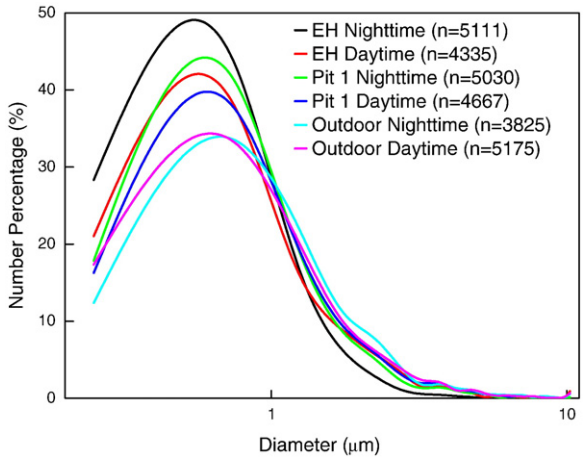

Fig. 4. Size distribution of airborne particles collected in EH, in Pit 1, and outdoors in the Museum at daytime and at nighttime, respectively. The diameter of each individual particle was measured from the SEM images.

free exchange of air masses through the opened windows in Pit 1, contributing higher percentage of particles with larger diameters. This is consistent with the result of mass concentration measurement since particle mass concentrations were controlled dominantly by coarse mode particles. The number percentage of particles smaller than 1.0 μm in EH at daytime was similar to that in Pit 1 due to identical tourist flow at opening time. The lowest percentages of daytime and nighttime fine particles were observed at outdoor sites.

3.4. Particle classification

3.4.1. Morphology

The particles were grouped into four dominant types according to their morphologies as soot aggregate, coal fly ash, mineral particles and other types with regular shapes. Fig. 5 shows the typical individual particles loaded on the filter at different magnifications from EH (Fig. 5a, d, e, and f) and Pit 1(Fig. 5b and c). As for particle numbers, mineral particles are the most frequently observed indoors, mainly derived from soil dusts and some other anthropogenic activities such as construction. Those mineral particles with irregular shapes (Fig. 5a and b) come either from entrainment by visitors and re-suspended particles inside the museum or from transport of fugitive dust around the museum. Elongate calcium sulfate and sodium sulfate particles (Fig. 5b and d) were probably formed by atmospheric reactions. Fly ash particles were normally smooth spheres (Fig. 5a) or spherical aggregates adhering to other particles (Fig. 5d) from coal combustion in BaHe thermo power plant 17 Km to the west of the Museum and a few local metallurgical factories. Soot aggregates were common in all the samples with two dominant morphological types: small chain of spherulites (Fig. 5e and f), and large clusters with a size of 1–5 um (Fig. 5a). It is suggested that the indoor soot particles in the Museum originated from a highway 5 km to the north. The Museum is located in a suburb environment, therefore biological particles (fragments of pollen or spore) were occasionally observed in indoor environment (Fig. 5c). Besides, some near spherical and near cubic particles remained unidentified. These indoor particles might be formed in a complicated way such as secondary particles from homogeneous chemical reaction or long range transport.

3.4.2. Elemental composition of particles

Before particles were measured, margins of polycarbonate filter (without particle loading) were detected and the average intensity (cps) was recorded as a threshold. When low-Z particles were detected under the same test conditions, the threshold value was adopted to differentiate particles from substrate. Low-Z particles with dominant C and O peaks in their spectra were designated as soot or biological particles, according to their particulate morphologies as soot consisting of chain or aggregate spheres and biogenic particles containing regular surface or symmetrical shapes. Identification of soil dust particles with dominant inorganic elements is based on their elemental compositions by excluding C and O peaks from the spectra (Okada and Kai, 2004) to avoid interference from the polycarbonate filter. The abundance of each element in each particle, $P(X)$, was calculated on the relative weight of each element divided by all ten most frequently detected elements. $P(X) = X/(\mathrm{Na}+\mathrm{Mg}+\mathrm{Al}+\mathrm{Si}+\mathrm{S}+\mathrm{K}+\mathrm{Ca}+\mathrm{Ti}+\mathrm{Mn}+\mathrm{Fe})$. Particles were classified into major "X-rich" or "X_1–X_2-…-X_N" group,

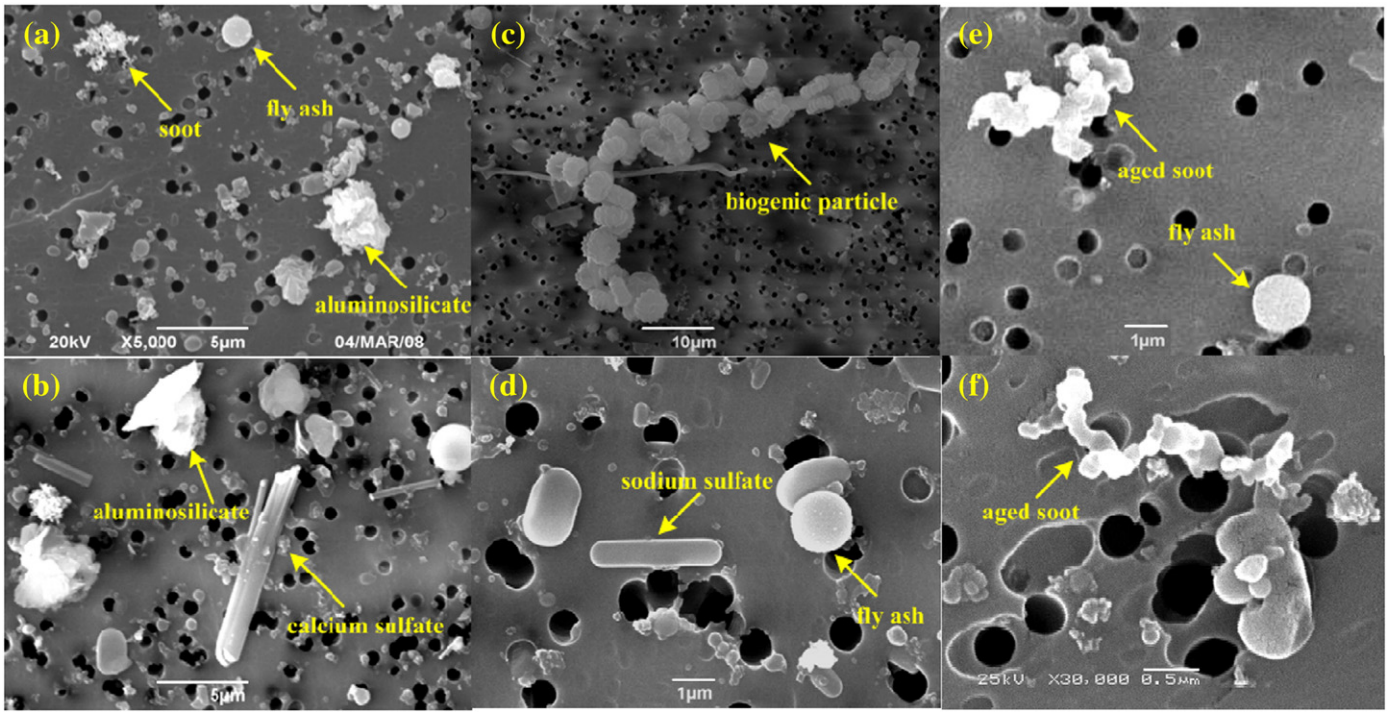

Fig. 5. Scanning electron micrograph of typical particles on Nucleopore filters collected in EH (a; d; e; f) and Pit 1(b; c).

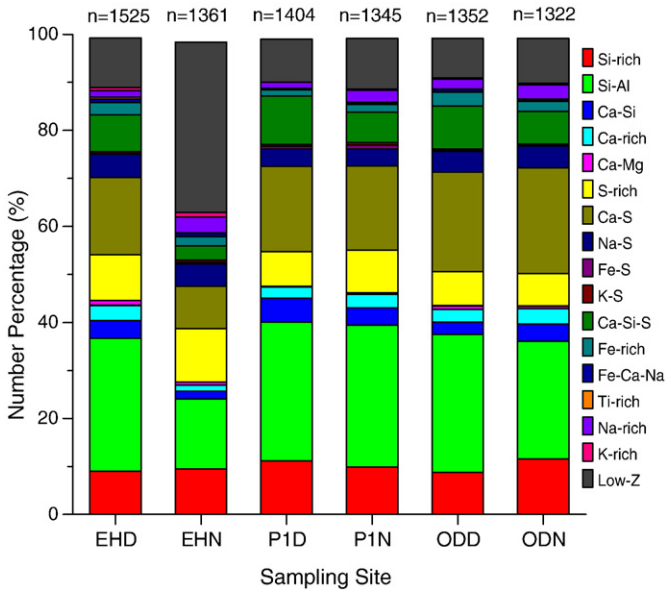

Fig. 6. Classification and number percentage of each sub-group in overall airborne particle samples collected in EH at daytime (EHD) and at nighttime (EHN), in Pit 1 at daytime (P1D) and at nighttime (P1N), and at outdoor site at daytime (ODD) and at nighttime (ODN).

where $P(X) \geq 0.65$, or $P(X_1) + P(X_2) + \ldots + P(X_N) \geq 0.65$. Using the 65% threshold, the particles were divided into several groups, and their number percentages were illustrated in Fig. 6. The sum of the abundance in Fig. 6 is not 100% because less than 2% particles in all the samples were unidentified particles with detectable elements that do not fall into any defined types and bias come from decreased volatile organic matter and nitrate compounds during sample preparation process under the vacuum environment. The exclusion of C and O also underestimates the organic content of particles.

Most of the "Si-rich" particles also contained Al, indicating these fugitive dusts from the Chinese Loess Plateau comprise quartz and clay minerals as montmorillonite, illite, chlorite, kaolinite, and muscovite (Wen, 1989; Eden et al., 1994; Kalm et al., 1996). Chinese loess is characterized as calcite-rich, with an average calcite content of 12.33% in the middle reaches of Yellow River (Wen, 1989) where the Museum located. Ca-containing particles contributed <5% of the total number with "Ca-rich" sub-group indicative of calcite, calces, calcium hydroxide and "Ca + Mg" sub-group indicative of dolomite. Other types such as "Fe-rich", "K-rich", and "Ti-rich" particles were summed less than 7% in all the samples. Although the highway traffic intensity at night was lower, outdoor abundances of soot particles kept stable during the sampling days probably due to higher emission of trucks at night than cars in the daytime.

The abundance of most daytime particle types are similar among all of the three sites, suggesting that the suspension and re-suspension of soil dust by visitor movement or nature ventilation, and transport of outdoor fugitive dust into the pit enclosures are the primary source of indoor TSP. Soil dust particles were present in high number fractions (>89%) in all samples except in EH at nighttime. More than 35% of the particles in EH at night were low-Z particles, mostly soot aggregate or aged soot with diameter smaller than 1 μm. Soot aggregate (Fig. 5a) was recognized by its characteristic morphology as an agglomeration of spherical particles with diameters between 20 and 100 nm. Aged soot (Fig. 5e and f) may lose their characteristic texture. The swollen links of spheres have grown together, but still with dendritic structure. No other element but carbon was detected in their EDX spectra. In EH, soil dust particles (normally >1 μm) stirred up by visitors during daytime partly deposited at night when the doors were closed. There was not enough time for the deposition of fine low-Z particles (normally <1 μm), resulting in their percentage increasing at night. Whereas in Pit 1, parts of the soil dusts were still transported by the natural ventilation through opened windows and retained all components at a stable level in both the daytime and nighttime.

Indoor soot and soil dust particles in the Museums are of particular interest because those species are light-absorbing and can produce visible soiling deposits on the statues. Coarse particles consist largely of soil dust and thus appear brown when deposited on a statue. Fine particles consist mostly of vehicle exhaust soot particles and are characteristically black or grey. Soil dust settles on upward-facing surfaces under the influence of gravity, whereas soot deposits to surfaces of any orientation by a combination of advective diffusion and thermophoresis (Nazaroff et al., 1993). Consequently, protection of terracotta statues from soiling due to the deposition of airborne particles includes alternative control measures, including employing mechanical ventilation and effective airborne particle filtration system, reducing the rate of induction of outdoor particles into the building, managing museum surrounding to achieve lower outdoor particle concentrations, and adopting proper pavement coverings and display strategy to reduce indoor particle sources due to visitor activities.

The number percentages of each type in the two display halls on the sampling day with the highest tourist flow (3439 persons on Feb 16) and those with the lowest visits (2186 persons on Feb 21) were summarized in Table 2. Abundance of Si-rich and Ca-rich particles was 36.2% on Feb 16, higher than that of 28.8% on Feb 21 in EH at daytime, indicating more coarse particles were stirred up and re-suspended by intensive tourist flow on Feb 16, a weekend day. The impact of an additional 57% of visitors on Feb 16 was indicated by the increased

Table 2
Classification and number percentage of each sub-group in daytime and nighttime samples collected in EH and Pit 1 on Feb 16 (highest visitor number) and on Feb 21 (lowest visitor number) in the sampling campaign.

Particle type	Number percentage (%)							
	Feb 16 (visitor number = 3439)				Feb 21 (visitor number = 2186)			
	EH-D[a] (196)[b]	EH-N[a] (178)[b]	Pit1-D[a] (184)[b]	Pit1-N[a] (178)[b]	EH-D[a] (229)[b]	EH-N[a] (204)[b]	Pit1-D[a] (202)[b]	Pit1-N[a] (193)[b]
Mass [c]	246.3	78.8	270.0	162.7	173.7	103.4	285.4	260.7
Low-Z	10.2	27.53	9.78	14.61	8.73	38.73	9.9	9.33
Si-rich	32.14	12.37	25.53	26.41	27.51	18.13	44.55	43.52
Ca-rich	4.08	1.69	5.43	2.81	1.31	0.98	2.97	1.04
S-containing	49.49	55.62	55.98	52.8	55.02	37.25	36.64	41.46
Fe-rich	2.55	2.25	1.09	1.12	2.62	0.98	1.49	1.55
Ti-rich	0	0	0	0	0.87	0.49	0	0.52
Mn-rich	0	0.56	0	0	0	0	0	0
K-rich	0.51	0	0	0	1.31	0.98	0	1.55
Total	98.98	100	97.83	97.75	97.38	97.55	95.54	98.96

[a] D means Daytime samples, N means Nighttime samples.
[b] Numbers in parentheses are the numbers of particles being detected in each sample.
[c] Unit is μg m^{-3}.

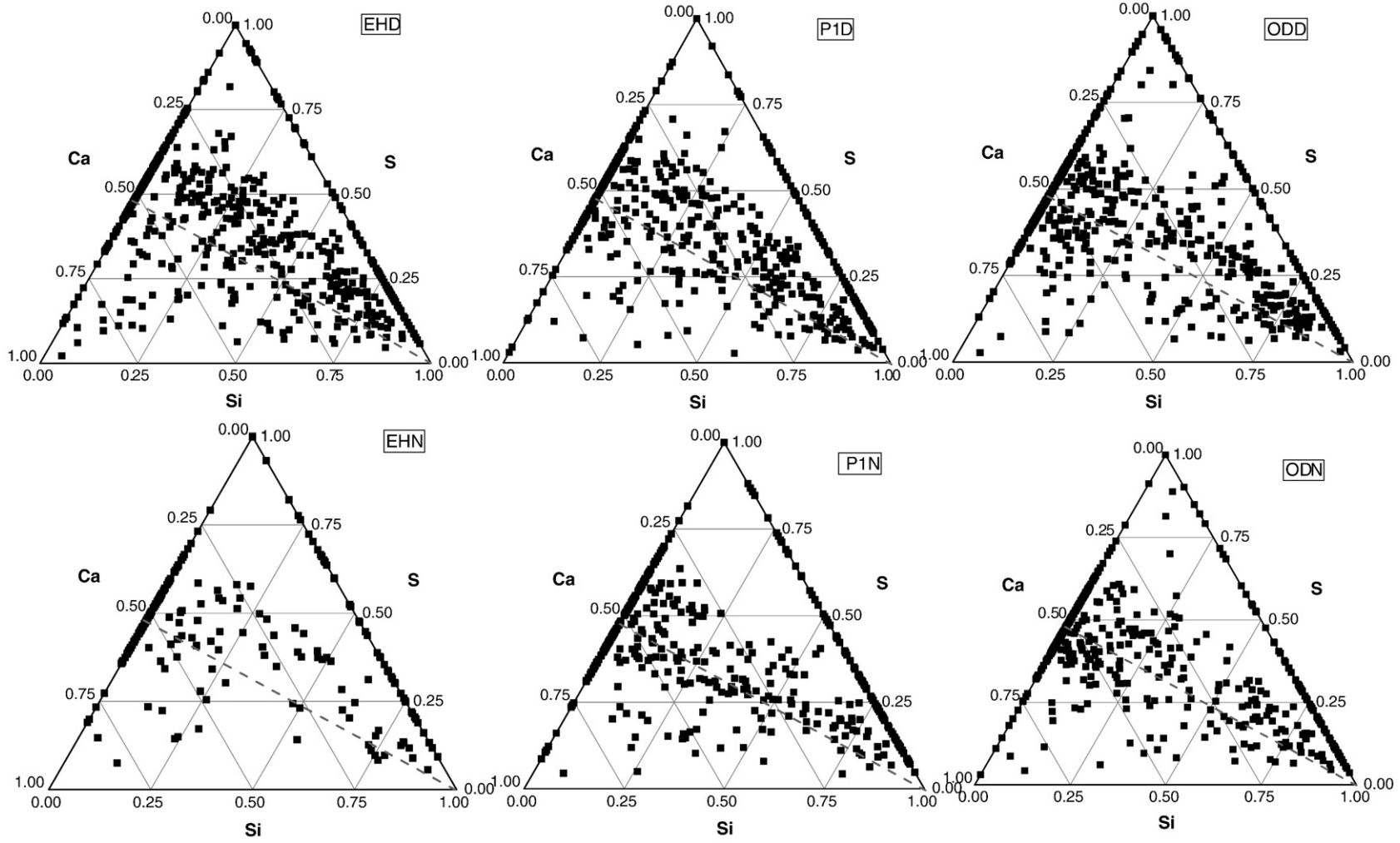

Fig. 7. Relative weight ratios of Si, S, and Ca for S-containing particles in EH at daytime (EHD) and at nighttime (EHN), in Pit 1 at daytime (P1D) and at nighttime (P1N), and at outdoor site at daytime (ODD) and at nighttime (ODN).

daytime abundance of soil dusts in EH. Without visitor activities at night, some of those coarse particles deposited, resulting in the higher daytime/nighttime abundance ratio of Si-rich and Ca-rich particles on Feb 16 (2.58) than that on Feb 21 (1.51). In Pit 1, the daytime/nighttime abundance ratios of Si-rich and Ca-rich particles were 1.06 on Feb 16 and 1.07 on Feb 21, respectively. Furthermore, higher percentages of soil dust were observed on the sampling day with fewer visitors, both at daytime and at nighttime, pointing to a larger impact of architectural and ventilating conditions on coarse mode soil dust particles in this display hall. In EH, the number percentages of low-Z particles at nighttime were 170% higher than that at daytime on Feb 16 and 344% higher than that on Feb 21. The increased abundance of low-Z particles, comprising mostly soot recognized by their characteristic morphologies, was owing to the decreased abundances of soil dust at night. The suspended low-Z particles need relative longer duration to deposit and their daytime/nighttime abundance ratios did not synchronize with the daily visitor numbers, implying that visitor numbers only played an important role on coarse soil dusts in EH. Study on indoor air quality in public buildings also found that PM_{10} (Guo et al., 2004) and CO_2 (Lee and Chang, 1999) may accumulate in air-conditioned buildings which were more sealed than the non-air-conditioned ones. It is also supported by the linear regression analysis of the 7-day daytime/nighttime mass ratios with visitor numbers. Although the R^2 value in EH (0.48) was higher than that in Pit 1 (0.10), the correlation between particle daytime/nighttime mass ratios and visitor flows in EH was weak, which can be explained by the long-term existence of suspended low-Z particles in the display halls.

3.4.3. S-containing particles

In addition to soiling by airborne particles, the deposited airborne material can attack statues resulting in physical and chemical weathering. Fig. 6 shows that S-containing particles were detected ranging from 28.3% in EH at night to 41.6% in outdoor TSP at daytime. In most sampling sites, "S + Ca" was the most abundant sub-group in S-containing particles, except "S-rich" particles was dominant in EH at nighttime. Among indoor and outdoor airborne particles, Ca-containing particles, including calcite ($CaCO_3$), calces (CaO), and dolomite ($CaMg(CO_3)_2$), were frequently detected. The "S + Ca" particles may be calcium sulfate formed by heterogeneous chemical reactions between atmospheric sulfur dioxide and Ca-containing particles. Since the mass ratio of Ca/S in gypsum, bassanite, and anhydrite is 1.25, a dashed line from the right corner to the left axis (Ca) was drawn on ternary plots of Si, S, and Ca elemental contents (Fig. 7). Particles distribute along this gypsum line indicating that gypsum particles were in an internally mixed state with clay or quartz, implying that soil dusts act as the carriers and/or reactants of those S-containing compounds. Since EDX data for element N was not available, the "S-rich" particles (shown by points near the S corner in Fig. 7) were assumed to be as ammonium sulfate or ammonium bisulfate. "S + Na" particles less than 5% in all the samples were possibly mirabilite and thenardite originated from anthropogenic emission or long range transport from dust region. "S + K" particles probably derived from fertilizer in the surrounding agricultural fields. A large number of "S + Fe" and "S + Ca + Si" particles had spherical morphologies, indicating their origin of coal combustion emission from the upwind power plant.

Salt weathering is one of the most important and common decay processes that affect materials such as rocks (Benavente et al., 2007), building stones (Cardell et al., 2003), brick (Cultrone et al., 2005), ceramics and concrete (Marinoni et al., 2003). Despite chemical reactions, damage caused by salts was classified into three types: crystallization pressure, hydration pressure, and differential thermal expansion (Kuchitsu et al., 1999), among which crystallization pressure of the salts could be the main threat to the surfaces. The harmful effects of soluble salts including sulfate presented in porous materials are mostly not in the form of solution but the formation of salt crystals and crystal-hydrates that often have crystallization pressures higher than the strength of the particular material (Nehdi and Hayek, 2005). In a previous study, crystals and floccules of calcium sulfate were observed near the edge of the pits and cracks on the surface of apatite lacquer pieces (calcium phosphate, $Ca_3(PO_4)_2$) in the Museum (Hu et al., 2006). According to the records between 1989 and 1992, the daily average temperature fluctuated from −4.2 °C to 32 °C in Pit 1, with daily average RH from 35% to 92% (Zhang, 1998). At higher RH, fine grains of sulfate can dissolve and penetrate into the inner pores of the statues. After evaporation of water, these salts recrystallize and cause stress, which may play an important role in the formation of pits and cracks on the surfaces of lacquer pieces.

4. Conclusions

SEM-EDX morphological and elemental analysis was utilized to characterize daytime and nighttime individual airborne particles collected inside two display halls with different structure and tightness and outside the Terra-cotta Museum in February 2008. The mass concentrations of ambient particles inside both of the sites remained at a high level. Size distribution and three types of particles showed soiling and physical weathering hazard due to visitor activities in Exhibition Hall and free air exchange in Pit No. 1. To protect the terra-cotta statues in the museum, appropriate measures should be deployed, including: employing mechanical ventilation and filtration system to reduce the infiltration of outdoor pollutants into the display halls; managing vegetation in the surrounding area to achieve lowered outdoor particle concentrations; adopting microclimate control measures to reduce fluctuations in temperature and humidity; regulating exhibiting strategies to reduce the induction of soil dust into the buildings and the abrasion of floors due to visitor movement.

Acknowledgements

This research was partially supported by the National Nature Science Foundation of China (40875089), the G-U330 Foundation (HKPU Joint Supervision Scheme with Mainland Universities 2006–2007), and the RGC project (Polyu 5204/07E).

References

Benavente D, Martínez-Martíneza J, Cuetoa N, García-del-Cura MA. Salt weathering in dual-porosity building dolostones. Eng Geol 2007;94:215–26.
Betzer PR, Carder KL, Duce RA, Merrill JT, Tindale NW, Uematsu M, et al. Long-range transport of giant mineral aerosol particles. Nature 1988;336:568–71.
Brimblecombe P. The composition of museum atmospheres. Atmos Environ 1990;24B(1):1–8.
Brimblecombe P. The effects of air pollution on the built environment. London: Imperial College Press; 2003. 63–175.
Cao JJ, Rong B, Lee SC, Chow JC, Ho KF, Liu SX, Zhu CS. Composition of indoor aerosols at Emperor Qin's Terra-cotta Museum, Xi'an, China, during summer, 2004. China Particuology 2005;3:170–5.
Cassar M, Blades N, Oreszczyn T. Air pollution levels in air-conditioned and naturally ventilated museum: a pilot study, In: Preprints of the 12th Triennial Meeting of the ICOM Committee for Conservation, Lyon. International Council of Museums 1999;1:31–7.
Cultrone G, Sidraba I, Sebastián E. Mineralogical and physical characterization of the bricks used in the construction of the "Triangul Bastion", Riga (Latvia). Appl Clay Sci 2005;28:297–308.
Camuffo D, Van Grieken R, Busse H, Sturaro G, Valentino A, Bernardi A, et al. Environmental monitoring in four European museums. Atmos Environ 2001;35: S127–40.
Cardell C, Delalieux F, Roumpopoulos K, Moropoulou A, Auger F, Van Grieken R. Salt-induced decay in calcareous stone monuments and building in a marine environment in SW France. Constr Build Mater 2003;17:165–79.
Dalia Pereira KC, Evangelista H, Bueno Pereira E, Simões JC, Johnson E, Melo LR. Transport of crustal microparticles from Chilean Patagonia to the Antarctic Peninsula by SEM-EDS analysis. Tellus 2004;56B:262–75.
De Bock LA, Van Grieken RE, Camuffo D, Grime GW. Microanalysis of museum aerosols to elucidate the soiling of paintings: case of the Correr Museum, Venice, Italy. Environ Sci Technol 1995;30:3341–50.
Eden DN, Wen Q, Hunt JL, Whitton JS. Mineralogical and geochemical trends across the Loess Plateau, North China. Catena 1994;21:73–90.
Germain MA, Hatton A, Williams S, Matthews JB, Stone MH, Fisher J, et al. Comparison of the cytotoxicity of clinically relevant cobalt–chromium and alumina ceramic wear particles in vitro. Biomaterials 2003;24:469–79.

Ghermandi G, Laj P, Capotosto M, Cecchi R, Riontino C. Elemental mineral characterisation of Coastal Antarctic aerosols in snow using PIXE and SEM-EDAX. Nucl Instrum Meth B 1999;150:392–7.
Godoi RHM, Kontozova V, Van Grieken R. The shielding effect of the protective glazing of historical stained glass windows from an atmospheric chemistry perspective: case study Sainte Chapelle, Paris. Atmos Environ 2006;40:1255–65.
Godoi RH, Potgieter-Vermaak S, Godoi AFL, Stranger M, Van Grieken R. Assessment of aerosol particles within the Rubens' House Museum in Antwerp, Belgium. X-Ray Spectrometry 2008;37:298–303.
Guo H, Lee SC, Chan LY. Indoor air quality investigation at air-conditioned and non-air-conditioned markets in Hong Kong. Sci Total Environ 2004;323:87–98.
Hu TF, Li XX, Dong JG, Rong B, Shen ZX, Cao JJ, et al. Morphology and elemental composition of dustfall particles inside Emperor Qin's Terra-cotta Warriors and Horses Museum. China Particuology 2006;4:346–51.
Ingham E, Green TR, Stone MH, Kowalski R, Watkins N, Fisher J. Production of TNF-α and bone resorbing activity by macrophages in response to different types of bone cement particles. Biomaterials 2000;21:1005–13.
Kalm VE, Rutter NW, Rokosh CD. Clay minerals and their paleoenvironmental interpretation in the Baoji loess section, Southern Loess Plateau, China. Catena 1996;27:49–61.
Kontozova-Deutsch V, Deutsch F, Godoi RHM, Spolnik Z, Wei W, Van Grieken R. Application of EPMA and XRF for the investigation of particulate pollutants in the field of cultural heritage. Microchim Acta 2008;161:465–9.
Kuchitsu N, Ishizaki T, Nishiura T. Salt weathering of the brick monuments in Ayutthaya, Thailand. Eng Geol 1999;55:91–9.
Lee SC, Chang M. Indoor air quality investigations at five classrooms. Indoor Air 1999;9:134–8.
Marinoni N, Birelli MP, Rostagno C, Pavese A. The effects of atmospheric multipollutants on modern concrete. Atmos Environ 2003;37:4701–12.
Nazaroff WW, Ligocki MP, Salmon LG, Cass GR, Fall T, Jones MC, Liu HIH, et al. Airborne particles in museums, Research in Conservation 6. Los Angeles: Getty Conservation Institute; 1993. 17.
Nehdi M, Hayek M. Behavior of blended cement mortars exposed to sulfate solutions cycling in relative humidity. Cement Concrete Res 2005;35:731–42.
Okada K, Kai K. Atmospheric mineral particles collected at Qira in the Taklamakan Desert, China. Atmos Environ 2004;38:6927–35.
Potgieter-Vermaak SS, Godoi RHM, Van Grieken R, Potgieter JH, Oujja M, Castillejo M. Micro-structure characterization of black crust and laser cleaning of building stones by micro-Raman and SEM techniques. Spectrochim Acta 2005;61:2460–7.
Sanchez-Morala S, Luquea L, Cuezvaa S, Solerb V, Benaventec D, Laizd L, Gonzalezd JM, et al. Deterioration of building materials in Roman catacombs: the influence of visitors. Sci Total Environ 2005;349:260–76.
Sheu JT, Chen CC, Huang PC, Hsu ML. Selective deposition of gold nanoparticles on SiO_2/Si nanowire. Microelectron Eng 2005;78–79:294–9.
Tansel B, Nagarajan P. SEM study of phenolphthalein adsorption on granular activated carbon. Adv. Environ Res 2004;8:411–5.
Thatcher TL, Layton DW. Deposition, resuspension, and penetration of particles within a residence. Atmos Environ 1995;29:1487–97.
Tian K, Thomson KA, Liu F, Snelling DR, Smallwood GJ, Wang D. Determination of the morphology of soot aggregates using the relative optical density method for the analysis of TEM images. Combust Flame 2006;144:782–91.
Trochkine D, Iwasaka Y, Matsuki A, Yamada M, Kim YS, Zhang D, et al. Comparison of the chemical composition of mineral particles collected in Dunhuang, China and those collected in the free troposphere over Japan: possible chemical modification during long-range transport. Water Air Soil Poll: Focus 2003;3:161–72.
Van Grieken R, Delalieux F, Gysels K. Cultural heritage and the environment. Pure Appl Chem 1998;70:2327–31.
Wen QZ. Chinese Loess Geochemistry. Beijing: Science Press; 1989. 1–158 pp. (in Chinese.
Worobiec A, Samek L, Karaszkiewicz P, Kontozova-Deutsch V, Stefaniak EA, Van Meel K, et al. A seasonal study of atmospheric conditions influenced by the intensive tourist flow in the Royal Museum of Wawel Castle in Cracow, Poland. Microchem J 2008;90:99-106.
Yoon YH, Brimblecombe P. Contribution of dust at floor level to particle deposit within the Sainsbury Centre for Visual Arts. Stud Conserv 2000;45:127–37.
Yoon YH, Brimblecombe P. The distribution of soiling by coarse particulate matter in the museum environment. Indoor Air 2001;11:232–40.
Yue W, Li X, Liu J, Li Y, Yu X, Deng B, et al. Characterization of $PM_{2.5}$ in the ambient air of Shanghai city by analyzing individual particles. Sci Total Environ 2006;368:916–25.
Zhang DZ, Zang JY, Shi GY, Iwasaka Y, Matsuki A, Trochkine D. Mixture state of individual Asian dust particles at a coastal site of Qingdao, China. Atmos Environ 2003;37:3895–901.
Zhang ZJ. Study on conservation of Qin Terra-cotta army. Xi'an: Shaanxi People Education Press; 1998. 1–159 pp. (in Chinese).